Effect of process parameters on strength and hardness of AA1100 fabricated by friction stir additive manufacturing

Ravinder Reddy Baridula*, *Jagadesh Kumar* Jatavallabhula, *Kukkala Surya* Manoj, *Pradeep Kumar* Juvvadi, and *K. Rajesh* Kumar

Department of Mechanical Engineering, Vidya Jyothi Institute of Technology, Aziznagar, Hyderabad, India

Abstract. This study investigates the process–property relationships in AA1100 aluminium alloy fabricated via Friction Stir Additive Manufacturing (FSAM), with a focus on optimising ultimate tensile strength (UTS) and Vickers microhardness through parameter tuning. A Taguchi L4 orthogonal array was employed to systematically vary tool rotational speed (900 and 1120 RPM), feed rate (25 and 40 mm/min), and tilt angle (1° and 2°), enabling quantitative analysis of main effects via analysis of means (ANOM). Results reveal that tilt angle is the most influential factor for UTS ($\Delta = 2.73$ MPa), with a 1° setting delivering the highest UTS of 91.89 MPa by promoting symmetric stirring and defect-free interlayer bonding. Conversely, rotational speed dominates hardness evolution ($\Delta = 1.2$ HV), where 1120 RPM enhanced dynamic recrystallization and yielded a peak average hardness of 36.63 HV. The UTS variation across runs was limited to approximately 3 MPa and hardness fluctuation was within 1.4 HV and this proved the process stability of FSAM for AA1100 and its capability to produce dimensionally and structurally consistent builds. The interplay between parameters highlights a trade-off: settings optimal for strength differ from those maximising surface hardness, necessitating application-specific process selection. These findings position FSAM as a viable, energy-efficient route for manufacturing dimensionally precise, mechanically stable, corrosion-resistant aluminium components, especially for aerospace, marine, and structural applications. Future work can focus on advanced microstructural characterisation, fatigue analysis and machine learning based predictive modelling for FSAM of aluminium alloys.

1 Introduction

AA1100 is a commercially pure aluminium alloy (≥99% Al) that has attracted considerable interest in engineering practice because it combines excellent corrosion resistance with superior formability and very good thermal and electrical conductivity. As a non-heat-treatable grade, it is particularly well suited to manufacturing processes that involve extensive plastic deformation, such as deep drawing, spinning, and stamping, while still maintaining

* Corresponding author: baridula@gmail.com

good surface finish and dimensional accuracy [1]. Its strong resistance to atmospheric and chemical attack, together with its naturally reflective surface, has led to widespread use in architectural cladding, insulation systems, chemical storage vessels, and reflective lighting fixtures. The high electrical and thermal conductivity further makes AA1100 a natural choice for conductors, bus bars, and heat exchangers in energy-efficient systems and lightweight thermal management applications. Although it is relatively soft and of modest strength, AA1100 continues to play an important role in aerospace, automotive, and marine components where ease of machining, corrosion tolerance, and recyclability are prioritised over high load-bearing capacity.

Friction Stir Additive Manufacturing (FSAM) is an additive welding process of solids based on the friction stir welding (FSW) [2]. In comparison to the old AM methods where the metal is melted, FSAM creates strong joints by the harsh plastic flow and the movement of atoms in the solid form. This results to small grains, reduction in the number of voids, and increase in the strength. A significant advantage is to deal with materials that are likely to crack during melting like hard types of aluminium or magnesium alloys or mixed metal systems. Since the amount of heat penetrating the part reduces, residual internal forces reduce considerably, minimizing warping. This is why it is applicable in aircraft, ships and also military systems that require a high degree of precise shapes and also stable durability. FSAM has also shown potential for producing functionally graded materials, repairing high-value parts, and fabricating thick-section components with tailored property distributions. In addition, its low energy demand and limited material wastage align well with emerging sustainability and resource-efficiency objectives in manufacturing.

Tao Yuan et al. investigated the influence of thermal cycling on the microstructure and mechanical properties of Al-6061 alloy builds fabricated by FSAM. They monitored real-time temperature histories and found that peak temperatures reached 408.2 °C, with thermal cycles increasing grain size from 2.7 μm (top) to 4.0 μm (bottom) and reducing dislocation density. Hardness and tensile strength declined from 74.6 HV and 248.21 MPa at the top to 68.7 HV and 231.42 MPa at the bottom, while vertical specimens showed poorer performance due to kissing bond defects. It was reported that microstructural inhomogeneity and mechanical property degradation were primarily driven by thermal cycling [3].

Zhang et al. examined the microstructural evolution and mechanical performance of wire + arc additive manufactured 2319 aluminium alloy during aging treatment. It was found that peak aging at 175 °C for 12 h produced optimal tensile strength (around 402 MPa) and hardness (around 134 HV) due to the formation of fine θ′ (Al2Cu) precipitates. Over-aging led to coarsening of θ′ phases and a consequent decline in properties. EBSD and TEM analyses revealed grain boundary precipitation, sub-grain formation, and a reduction in dislocation density with aging time. The study concluded that precise control of aging parameters was critical to achieving balanced strength and ductility in WAAM 2319 alloy builds [4].

Chaudhary et al. investigated the influence of feedstock form and T6 heat treatment on the microstructure, deposition efficiency, and mechanical performance of FSAM manufactured Al 6061 alloy multilayers. It was reported that untreated powder-form depositions exhibited finer grains, lower porosity, and better strength than rod-form counterparts, while heat-treated rod-form depositions achieved higher strength due to dense Mg2Si precipitates despite higher porosity. Heat treatment evidently increased yield and tensile strengths for both feedstock forms but reduced ductility, shifting fracture behaviour from ductile to mixed brittle-ductile. Powder feedstock yielded 40% higher deposition efficiency, finer surface finish, and higher deposition temperature, whereas rod feedstock produced greater layer height in fewer passes [5].

Bozkurt et al. have extensively reviewed FSAM to aerospace alloys and have highlighted its obvious benefits relative to fusion-based AM of eliminating solidification defects and permitting the formation of fine-grained and virtually defect-free structures. Meanwhile, they identified some significant limitations that continue to impede its industrial implementation, including the challenge in producing highly complicated shapes and the lack of information regarding its functioning at dynamic load. Comprehensively, it was found in the review that FSAM is a very promising path towards producing lightweight aerospace components, although more research needs to be done on fatigue, impact resistance, and thermal cycling behaviour before realisation of large-scale implementation is achievable [6].

Hassan et al. discussed FSAM within the wider scope of non-ferrous alloys, its mechanism of operation in the solid state, reasons why it is superior to melting-based AM paths, and the applications in multi-layer laminates with fine microstructures. Their review systematically addressed the effect of machine settings, tool design and material parameters on the resultant properties and defects. They also summarised the most common types of the flaws, along with the methods of reducing them, as well as provided an overview on the technology preparation, the applications of the technology, and the probable research direction in the future [7].

Mishra et al. placed FSAM and additive friction stir deposition (AFSD) as solid state alternatives to traditional fusion-based AM, in the whole range of aluminium, titanium, magnesium, steels, and Ni based superalloys. It has suggested a systems-level process modelling framework, and the possibility of using machine learning to optimise process parameters. They have also noted a number of significant limitations or problems that include tool wear, geometric resolution limitation and process monitoring gaps, which require their resolution later in the research [8]. More in line with these advances, Roodgari et al. revealed that FSAM is able to produce high quality metallurgical bonding in a two-layer laminated steel composite and that further supports the fact that this process is capable of multilayer fabrication [9].

Despite substantial progress on FSAM for aluminium alloys, most existing studies concentrate on precipitation-hardenable grades such as AA6061, where post-process heat treatment is a key lever for improving properties. In contrast, there is a clear lack of systematic work on non-heat-treatable, commercially pure alloys like AA1100, especially when it comes to disentangling the individual and combined effects of key process parameters like tool rotational speed, feed rate, and tilt angle on the resulting mechanical properties. Experimental data that directly link these parameters to process stability and defect-free layer consolidation in FSAM-built AA1100 components are also limited. Closing this gap is important if AA1100 is to be more widely used in lightweight, corrosion-resistant structural applications where both tensile strength and surface hardness matter. Accordingly, the present work aims to:

- Fabricate multilayer AA1100 aluminium alloy components using FSAM under systematically varied processing conditions.
- Evaluate the influence of tool rotational speed, feed rate, and tilt angle on UTS and Vickers microhardness.
- Employ Taguchi L4 orthogonal array and analysis of means (ANOM) to identify the most influential parameters and optimal settings for both UTS and hardness.

2 Materials and methods

2.1 Material

The material used in this study is AA1100, an industrial, commercially pure aluminium alloy with a minimum aluminium content of ≥99.0 wt.% [10]. Unlike heat-treatable grades, AA1100 is particularly attractive for solid-state processes because of its high ductility, low flow stress, and excellent thermal conductivity. These attributes are also highly beneficial in friction-based additive layer fabrication. Its chemically simple composition promotes stable plastic flow during stirring, while the absence of hard intermetallic phases helps to limit tool wear and reduces the risk of interlayer defects. These characteristics make AA1100 a strong candidate for FSAM, where robust material bonding and reliable layer consolidation depend on tight control of thermomechanical conditions. In addition, traces of Fe, Si, and Cu that are present within narrow specification limits support dimensional stability and reduce susceptibility to hot cracking. This helps in preserving the microstructural uniformity across successive layers. The detailed chemical composition of AA1100 is reported in Table 1, and the base plates (100 mm × 50 mm × 2 mm) used for the FSAM process are shown in Fig. 1. Three plates are joined together as part of the FSAM so that the thickness of the final sample is 6 mm.

Table 1. Chemical composition of AA1100.

Element	Composition (wt.%)
Aluminium (Al)	99.0
Copper (Cu)	0.05-0.20
Iron (Fe)	0.0-0.95
Silicon (Si)	0.0-0.95
Zinc (Zn)	0.0-0.1
Manganese (Mn)	0.0-0.05

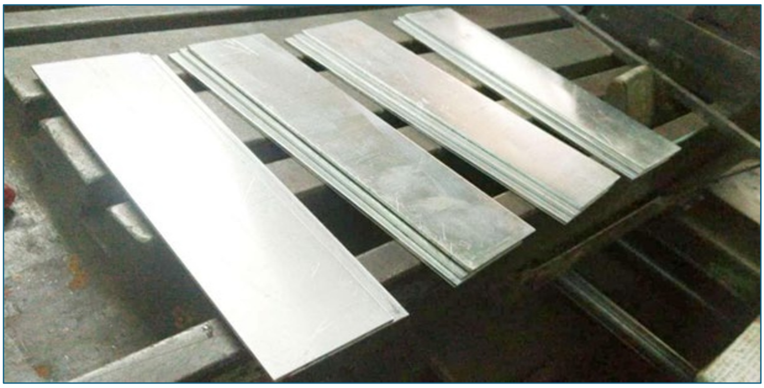

Fig. 1. Plates of AA1100 used for FSAM process.

2.2 FSAM machine

A vertical HMT milling machine equipped with an automated feed system (Figure 2) was adapted to perform the FSAM trials. The tool rotational speed and feed rate were chosen and optimized according to the previous research and initial process testing to achieve defect free additive layers. It was decided to use a tapered pin tool since it is able to produce sufficient frictional heat and allows the plasticised material to flow smoothly as it is deposited.

The tool shoulder was aimed at providing a tangential compressive force, which helps to consolidate the material and keep the layer height constant. Altogether, it is possible to notice that the tapered pin design is especially useful in FSAM because it promotes the mixing of the materials, minimizes the occurrence of a tunnel type defect, and leads to an enhanced performance in the area of mechanics in the end product. The integrated machine system, together with the tool geometry, was hence the primary concern in the production of multilayer joints that have good structural integrity.

Fig. 2. Vertical milling machine modified to perform the FSAM.

2.3 Detail of the tool

H13 tool steel is used for the tool of the FSAM machine. It is a chromium-molybdenum-based hot work alloy widely employed in precision die and tooling applications due to its outstanding combination of thermal fatigue resistance, mechanical toughness, and hot hardness [11]. Characterized by a microstructure enriched with approximately 12% chromium, it exhibits a ledeburitic morphology that contributes significantly to its superior wear resistance under high-stress, high-temperature conditions. Typical industrial applications include shear and trimming dies, blanking tools for polymeric and paper-based materials, rotary shear blades for sheets up to 2 mm in thickness, and cutting tools designed for metal sheets up to 4 mm, where dimensional stability and tool longevity are critical. The geometric details of the tool are presented in Table 2 and the actual tool is illustrated in Figure 3.

Table 2. Details of the tool.

Geometric parameter	Dimension
Shank diameter	18 mm
Diameter of shoulder	24 mm
Shape of pin	Taper
Diameter of pin	6-8 mm
Length of pin	5.8 mm

Fig. 3. Tool used for FSAM process.

2.4 Tensile testing

Tensile testing was carried out on a computerized Universal Testing Machine (UTM) of 100 KN capacity supplied by Fine Manufacturing Group. Figure 4 illustrates the dimensional profile of the tensile specimen employed for evaluating the mechanical response of FSAM-fabricated AA1100 plates. The specimen geometry adheres to the ASTM E8/E8M standard and Wire Electrical Discharge Machining (Wire EDM) was chosen for specimen fabrication due to its high dimensional fidelity and negligible thermal influence, which preserves the microstructural integrity of the HAZ. This is particularly crucial for FSAM builds, where residual stress gradients and layer-wise thermal histories may influence localized mechanical behaviour. DK 7735 Wire EDM machine supplied by SN Enterprises was utilized for precision cutting of the tensile testing specimens. For each test condition, at least three specimens were tested so as to report the average of best three results for ensuring repeatability and reliability.

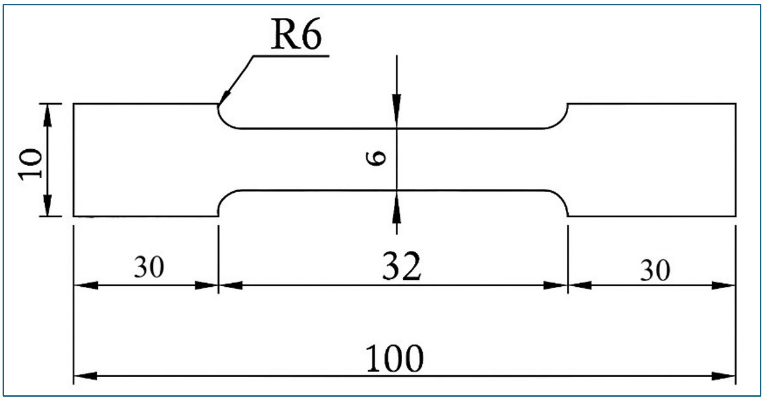

Fig. 4. Tensile specimen geometry.

2.5 Hardness testing

Vickers microhardness testing was carried out to characterise the surface and near-surface mechanical response of the FSAM-fabricated AA1100 specimens. A calibrated digital microhardness tester was used with a 500gf load and a dwell time of 15s, following ASTM E384. Each build was sectioned perpendicular to the build direction using wire EDM to avoid thermal damage and preserve dimensional accuracy.

To capture possible variations arising from layer-wise thermal cycling and recrystallisation, hardness measurements were taken at three vertical positions in each specimen: the bottom (Layer 1), middle (Layer 2), and top (Layer 3). At least three valid indentations were made at each layer, and the average value was reported to ensure statistical robustness and good repeatability. The resulting hardness profiles provide insight into how process parameters, particularly rotational speed, feed rate, and tilt angle affect local strain hardening and microstructural evolution within the deposited regions.

2.6 Design of experiments

A Taguchi-based Design of Experiments (DoE) strategy was employed in order to investigate the influence of the main process parameters on the mechanical behaviour of AA1100 fabricated by FSAM. The reasons why three factors were selected are that high rotational speed of the tool (r, RPM), high feed rate of the tool (f, mm/min), and high tilt angle of the tool (t, degrees) significantly affect the material flow and interlayer bonding. All of them were researched on two levels (low and high) as shown in Table 3. The chosen ranges have been in accordance with those used in previous FSAM literature [5-7], in which they have been demonstrated to give rise to stable interlayer bonding, refined microstructures, sufficient material flow and controlled heat input. Related FSW/FSP studies on AA1100 have also indicated that rotational speeds around 1120-1140 rpm favour grain refinement via dynamic recrystallisation [12, 13], further supporting these choices as a reliable process window.

An L4 orthogonal array (Table 4) was used to design the experiments, allowing the main effects of each factor to be evaluated efficiently with a minimal number of trials. All four runs were carried out under the same ambient conditions and machine setup to maintain consistency. The measured responses, ultimate tensile strength (UTS) and Vickers hardness (HV) were then examined using response tables and Analysis of Means (ANOM) to quantify the relative influence of each parameter and identify their optimal settings.

Table 3. Factors chosen and their levels.

Factor	Notation	Units	Level	
			Low	High
Tool Rotational Speed	r	RPM	900	1120
Tool Feed Rate	f	mm/min	25	40
Tool Tilt Angle	t	degrees	1	2

Table 4. Taguchi L4 array of experimental runs.

r	f	t
900	25	1
900	40	2
1120	25	2
1120	40	1

3 Results and discussion

Figure 5 illustrates the FSAM process in action during the deposition of successive layers on AA1100 substrates. As the rotating tool engages with the aluminium plate, localized frictional heating and intense plastic deformation are generated, but the temperature remains below the melting point. In this softened state, the material is stirred and consolidated under the tool shoulder, undergoing dynamic recrystallisation and giving rise to a fine-grained microstructure.

The tapered pin tool used in this study helps to maintain smooth material flow and reduces the likelihood of typical defects such as tunnel voids or incomplete bonding between layers. A stable plasticised zone develops around the tool, visible as a heat-affected region (HAZ), and this zone is crucial for achieving sound metallurgical bonding and uniform layer build-up. The observed surface finish and controlled flash formation indicate that the heat input and tool plunge depth were appropriately selected, both of which are key to producing defect-free components in solid-state AM.

Fig. 5. AA1100 plates being welding.

Figure 6 represents the four AA1100 plates, which have passed the FSAM process. In all specimens, the appearance of the surface is quite homogeneous, and flash or visible flaws in the surface are minimal, suggesting that the tool shoulder was in a good balance with the workpiece when it comes to heat input and forging effect. Such a uniformity of all runs is indicative of a strong process window, specifically concerning the selected tool tilt angle and rotational velocity, which can regulate material movement, heat production and consolidation of layers. The fact that there are no visible macro-defects, such as surface tunnels, interlayer spacing, or unbonded areas also contributes to the efficiency of the tool to tapper pin in ensuring complete stirring and reducing the possibility of local thermal or flow variations.

Fig. 6. The four AA1100 plates after welding.

3.1 Optimization of UTS

Figure 7 illustrates tensile samples cut out of each FSAM-fabricated plate of AA1100 with the highest precision wire EDM that served to reduce dimensional error and prevented thermal damage. The stable geometry in all the four samples shows that the FSAM process is stable and indicates the appropriateness of AA1100 in solid-state AM given the correct tool-path parameters. It is worth noting that in all of the process conditions no macroscopic evidence of delamination, incomplete bonding or visible porosity was detected in any specimen, which indicates that there is good metallurgical consolidation along the build direction. The clean edges and smooth uniform edges of the gauge sections and the accuracy with which the operation of cutting the wire were executed also indicated good as-deposited build quality.

(a)

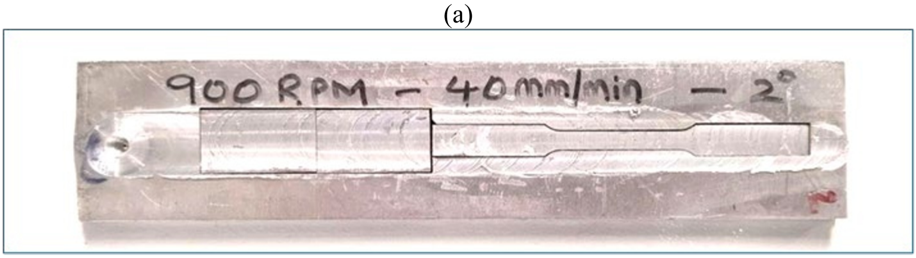

(b)

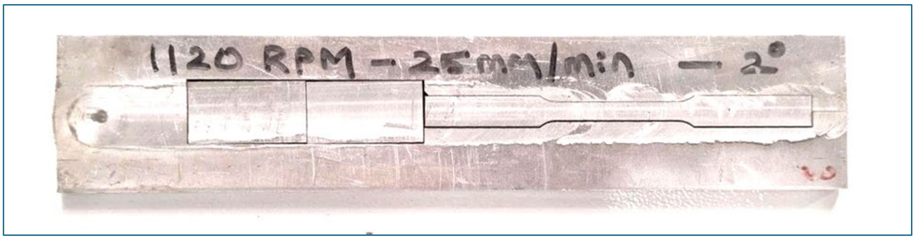

(c)

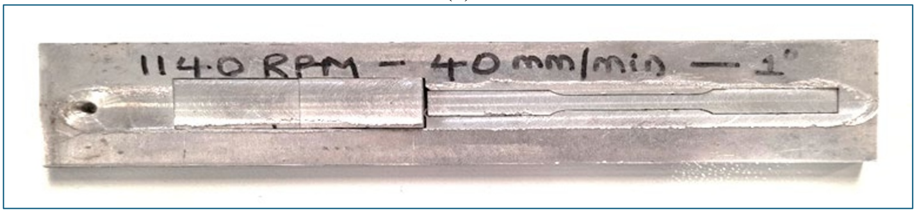

(d)

Fig. 7. Tensile specimens fabricated from Wire EDM, (a) Run 1, (b) Run 2, (c) Run 3, (d) Run 4.

Table 5 highlights the measured values of UTS for each FSAM-fabricated specimens as a function of the three most significant variables namely, tool rotation speed (r), feed rates (f), and tilt angles (t). The maximum values of UTS were observed in Runs 1 & 4, which measured 91.89 MPa & 91.23 MPa, respectively. Runs 2 & 3, which have involved either higher values of (f) or higher values of (t), showed slightly reduced values for UTS, measured between 88.70-88.95 MPa, due to reduced material mixing efficiencies or improper heat distribution, respectively. Taking into consideration the measured values of UTS, it is clear that they vary by approximately only 3 MPa, which, despite excluding all experimental runs, is a clear index of high FSAM process stability as well as low defect dispersions, thus collectively validating efficacy of FSAM as a reliable process for the fabrication of industrial-grade aluminium alloys. The trends of these results mirror those reported for Al-6061 where it was reported that tilt angle governs interlayer flow/bonding and hence UTS [3, 6].

Table 5. UTS results from tensile testing.

Run	r	f	t	UTS (MPa)
1	900	25	1	91.89
2	900	40	2	88.70
3	1120	25	2	88.95
4	1120	40	1	91.23

Fractured specimens of tensile testing are depicted in Figure 8 and they exhibited typical ductile fracture features such as necking and uniform elongation across the gauge length, consistent with the high ductility of commercially pure AA1100. No signs of interlayer delamination or lack-of-fusion defects were observed along the fracture path, indicating that the FSAM process produced strong metallurgical bonding between successive layers. These observations support the tensile data by confirming that failure occurred through bulk material ductile rupture rather than through weak interlayer interfaces, thus evidencing the integrity of the additive bonding.

Fig. 8. Tensile specimens after failure.

Table 6 provides a statistical breakdown of the mean UTS values corresponding to different levels of the FSAM process parameters, derived using the Taguchi method. The analysis shows that tool tilt angle (t) is the dominant factor, with a delta of 2.73 MPa, much larger than that of feed rate (0.45 MPa) and rotational speed (0.21 MPa). This shows that slight shifts in tilt angle greatly impact HAZ dimensions, material movement patterns, also interfacial bond quality. A 1° tilt gave higher UTS, at improved tool-to-workpiece contact, which supports balanced mixing plus sound layer joining. On the other side, steeper angles may disrupt metal flow routes as well as trigger uneven heating, thus undermining adhesion and lowering tensile performance. The smaller effect of Feed rate comes from its control over exposure duration along with thermal accumulation; meanwhile, rotation speed had limited outcome across trials, suggesting the energy delivered by friction stays adequate within this setup.

Table 6. Response table of means for UTS.

Level	r	f	t
1	90.30	90.42	91.56
2	90.09	89.97	88.83
Delta	0.21	0.45	2.73
Rank	3	2	1

Figure 9 illustrates the shift of ultimate tensile strength alongside individual processing variables. Although rotation speed displays an almost horizontal pattern, implying minimal influence from spindle velocity across tested levels, feed rate presents a gentle decline, suggesting faster movement could impair material mixing slightly. In comparison, increasing tilt angle leads to a noticeable reduction in strength, highlighting its key impact on layer adhesion and thermal balance during fabrication. Table 6 quantifies these influences numerically while the ANOM plot in Figure 9 offers a more direct, visual means of pinpointing the parameter levels that favour higher UTS.

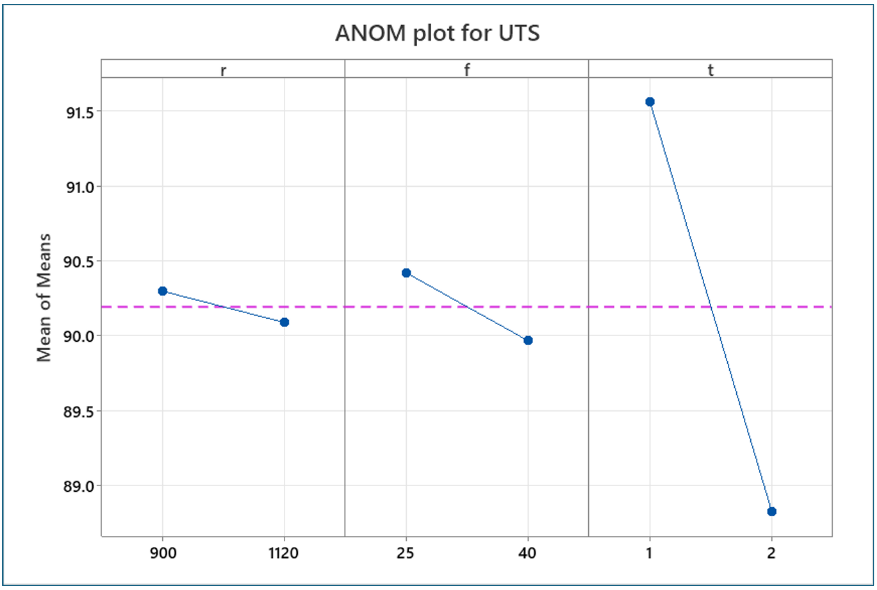

Fig. 9. ANOM plot for UTS.

ANOVA results of UTS presented in Table 7 re-confirm that tilt angle overwhelmingly controls UTS, contributing 96.78 % of the total variance, while feed rate and rotational speed contribute only 2.66 % and 0.57 %, respectively. Although the L4 design leaves no residual degrees of freedom, these relative contributions clearly establish tilt angle as the dominant factor governing interlayer flow and bonding, complementing the mean-response trends in Table 6 and the ANOM plot in Figure 9.

Table 7. ANOVA results of UTS.

Source	DOF	SS	MS	% Contribution
r	1	0.04368	0.04368	0.57
f	1	0.20521	0.20521	2.66
t	1	7.47476	7.47476	96.78
Error	0	--	--	--
Total	3	7.72365	--	--

3.2 Optimization of hardness

Figure 10 shows the specimens sectioned from each FSAM-fabricated AA1100 plate for microhardness evaluation across three distinct build layers. Table 8 summarizes the Vickers hardness values recorded at each layer, with averages ranging from 35.20 HV to 36.63 HV across all experimental runs. The hardness values remained relatively consistent, yet a noticeable upward trend was observed in specimens fabricated at higher tool rotational speeds and feed rates. The results are in agreement with those that documented AA6061, in which tool rotation speed was observed to affect the generation of frictional heat, dynamic recrystallization, grain refinement, and hardness [5,7]. For this study, Run 4, involving a speed of 1120RPM, feed of 40mm/min, and a tilt of 1°, showed an average hardness of 36.63 HV, which is higher than in previous runs. The result for hardness in Run 3, at 36.37 HV, also supports this result, as although the machine's tilt is higher at 2°, dynamic recrystallization due to greater heat input at higher speeds facilitates increased hardness in this zone.

In comparison, Run 1 (900 RPM, 25 mm/min, 1° tilt) had the lowest mean hardness, 35.20 HV, indicating less heat buildup along with smaller plastic deformation, factors linked to larger grains forming as the material cools. Looking at different levels, Layer 2 was harder than Layers 1 and 3 in three out of four cases throughout the vertical section. That points to middle layers gaining advantages due to repeated thermal exposure combined with physical mixing when later layers are added, where these combined actions improve structural fineness.

Overall, hardness changes slightly across settings, only around 1.4 HV, yet patterns show how rotation speed along with feed rate influence microstructure in FSAM parts. No sudden shifts in hardness from layer to layer suggest steady processing, minimal temperature differences, also uniform energy delivery. Such factors support structural consistency in additive manufacturing. Comparing these hardness findings with ultimate tensile strength data reveals that using a small tilt angle (1°), paired with medium-high rotation plus travel speeds, creates a favourable range where both strength and surface resistance improve, making it possible to produce dependable AA1100 components through FSAM.

Fig. 10. Hardnes specimens sectioned from the FSAM-fabricated AA1100 plate.

Table 8. Hardness results.

Run	r	f	t	Vickers microhardness (HV)			
				Layer 1	Layer 2	Layer 3	Average
1	900	25	1	35.1	35.3	35.2	35.20
2	900	40	2	35.5	35.1	35.6	35.40
3	1120	25	2	36.4	37.4	35.3	36.37
4	1120	40	1	36.8	37.5	35.6	36.63

Table 9 quantitatively compares the mean hardness values corresponding to each level of the FSAM process parameters. The impact of rotation speed stands out clearly showing a 1.2 difference across settings, suggesting faster RPM boosts grain refinement due to greater friction heat while enhancing dynamic recrystallization. Consistent with prior studies on solid-state joining of mild aluminum alloys, increased tool velocity results in smaller grains and improved hardness via stronger thermal and mechanical mixing. In contrast, feed rate affects hardness less strongly ($\Delta = 0.23$), tied mainly to how it regulates contact duration and cooling. Slower feeds prolong tool material engagement, supporting enhanced densification along with more pronounced strain-induced strengthening.

In contrast, the tilt angle shows only a marginal effect ($\Delta = 0.03$), suggesting that within the tested range (1°-2°), its impact on surface microhardness is negligible, quite different from its dominant role in UTS optimisation. Taken together with the layer-wise hardness consistency reported in Table 8, these results highlight rotational speed as the primary parameter governing surface and near-surface mechanical response in FSAM-fabricated AA1100.

Table 9. Response table of means for hardness.

Level	r	f	t
1	35.3	35.78	35.92
2	36.5	36.02	35.88
Delta	1.2	0.23	0.03
Rank	1	2	3

Figure 11 shows the ANOM plot for microhardness, providing a visual counterpart to the statistical trends reported in Table 9. The upward trend with increasing rotational speed confirms its leading influence on surface hardness, driven by higher frictional heat generation and more pronounced dynamic recrystallisation at elevated RPMs. The slight increase in hardness with feed rate indicates that slower traverse speeds, which extend the tool-workpiece interaction time, support improved plastic flow and more effective layer consolidation.

By contrast, the almost flat response associated with tilt angle over the 1°-2° range suggests that its effect on microhardness is minimal, indicating that the thermal-mechanical changes introduced by small variations in tool inclination do not significantly alter the near-surface hardness of AA1100. Taken together, the ANOM plot makes it straightforward to visually identify favourable processing conditions: higher rotational speeds combined with moderate feed rates emerge as the most suitable combination for maximising surface hardness in FSAM builds. Unlike UTS, where tilt angle played a decisive role, hardness is governed mainly by thermal and strain-rate-related effects, underscoring that different mechanical properties respond to distinct aspects of the process.

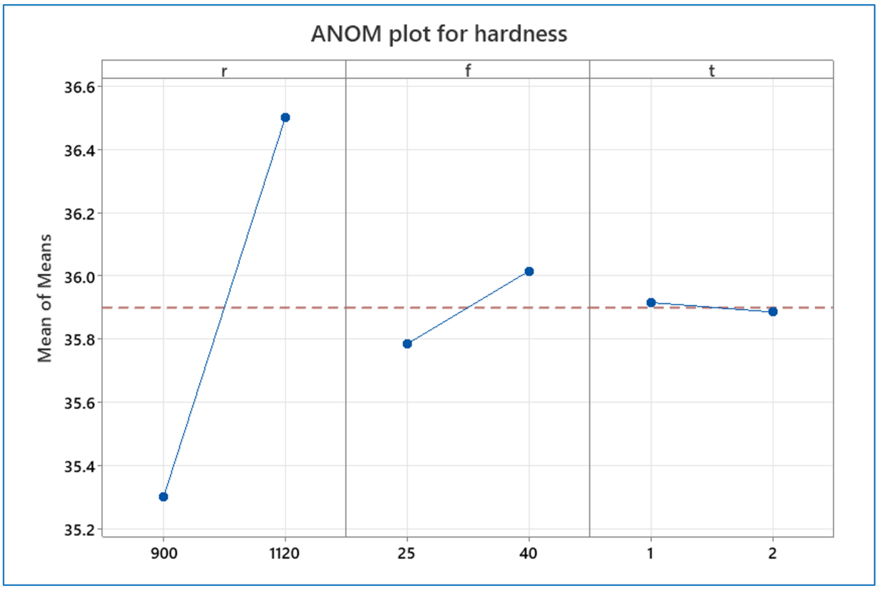

Fig. 11. ANOM plot for hardness.

ANOVA results of hardness (Table 10) reconfirm that tool rotational speed is the dominant factor controlling hardness, accounting for about 96.4 % of the total variance, while feed rate and tilt angle contribute only 3.54 % and 0.06 %, respectively. These findings complement the mean-response trends in Table 9 and the ANOM plot in Figure 11, underscoring that hardness in FSAM-fabricated AA1100 is primarily governed by thermal-mechanical effects of tool speed.

Table 10. ANOVA results of hardness.

Source	DOF	SS	MS	% Contribution
r	1	1.44	1.44	96.40
f	1	0.0529	0.0529	3.54
t	1	0.0009	0.0009	0.06
Error	0	--	--	--
Total	3	1.4938	--	--

3.3 Metallurgical rationale for parameter influence

The dominant influence of tilt angle on UTS can be linked to its direct control over interlayer material flow and heat distribution. A smaller tilt angle promotes more symmetric plasticised flow beneath the tool shoulder, leading to uniform metallurgical bonding and reducing the likelihood of kissing-bond defects, thereby improving tensile strength [3, 6]. In contrast, the stronger impact of rotational speed on microhardness stems from its role in frictional heat generation and strain rate: higher RPM intensifies local thermo-mechanical stirring and dynamic recrystallisation, refines the grain structure, and consequently raises near-surface hardness [5, 7, 14].

4 Conclusions

This study examined how three key FSAM process parameters, namely tool rotational speed, feed rate, and tilt angle affect the tensile strength and microhardness of AA1100 components. The results establish clear links between processing conditions and mechanical response, offering a basis for optimising solid-state additive manufacturing of non-heat-treatable aluminium alloys. The main conclusions are:

- Taguchi analysis showed that tool tilt angle is the dominant factor for UTS, with a Δ of 2.73 MPa, far exceeding the influence of feed rate (Δ = 0.45 MPa) and rotational speed (Δ = 0.21 MPa). In contrast, microhardness was governed primarily by rotational speed (Δ = 1.2 HV), with a smaller contribution from feed rate, while tilt angle had a negligible effect.
- The maximum UTS (91.89 MPa) was obtained at 900 RPM, 25 mm/min feed, and 1° tilt, whereas the highest average hardness (36.63 HV) occurred at 1120 RPM, 40 mm/min, and 1° tilt. This divergence indicates that the parameter set that maximises strength is not identical to that which maximises surface hardness, and that practical applications will require a trade-off depending on performance priorities.
- Both UTS and hardness showed only modest variation across the experimental runs (about 3 MPa for UTS and 1.4 HV for hardness). This low scatter reflects the intrinsic stability of the FSAM process for AA1100 and its ability to deliver builds that are dimensionally and structurally consistent.
- The strong dependence of UTS on tilt angle underscores the importance of symmetric material flow and balanced heat distribution for sound metallurgical bonding. Conversely, the sensitivity of hardness to rotational speed highlights the central role of frictional heating and dynamic recrystallisation in near-surface strengthening. These trends are consistently supported by both ANOM and ANOVA.

- The demonstrated capability to produce defect-free, mechanically uniform AA1100 structures through appropriate parameter control confirms FSAM as a scalable, sustainable, and industrially attractive solid-state AM route for lightweight, corrosion-resistant aluminium components.

This study identifies a feasible processing range combining mechanical strength with surface hardness, providing actionable insights for using AA1100 in light yet stable components like ship parts, cooling systems, or aircraft outer layers. Follow-up research may expand this base by examining internal structure features, testing durability under cyclic loads, or applying data-driven models to forecast behaviour of friction stir additive manufactured aluminium alloys.

References

1. L. Li, C. B. Smith, and K. A. Ross, "Constitutive model development of aluminum alloy 1100 for elevated temperature forming process," *The International Journal of Advanced Manufacturing Technology*, vol. **133**, pp. 1201-1216, (2024). https://doi.org/10.1007/s00170-024-13743-0
2. Baridula RR, Ramaraju RV, Ibrahim AB, Ku MF, "Effect of nano particle deposition on mechanical properties of friction stir welded dissimilar aluminium alloys by Taguchi technique," *Transactions of the Indian Institute of Metals*, vol. **70**, no. 4, pp. 1005-1017, (2017).https://doi.org/10.1007/s12666-016-0898-4
3. T. Yuan, Y. Sha, S. Wang, S. Yang, C. Zhao, H. Shan, and S. Chen, "Microstructure evolution and mechanical properties of friction stir additive manufacturing for Al-6061 alloy builds under thermal cycling," *Journal of Alloys and Compounds*, vol. **1027**, Art. no. 180559,(2025). https://doi.org/10.1016/j.jallcom.2025.180559
4. Y. Zhang, X. Guan, L. Wang, X. Wang, and X. Zhan, "The microstructure diversity in different areas of the ring-route Al 6061-T6 additive zone by friction stir additive manufacturing," *The International Journal of Advanced Manufacturing Technology*, vol. **128**, pp. 4857-4871, (2023) .https://doi.org/10.1007/s00170-023-11882-4
5. B. Chaudhary, N. K. Jain, J. Murugesan, and D. Sathiaraj, "Study of microstructure evolution and mechanical properties in friction stir based additive multi-layer manufacturing of Al 6061 alloy: Effect of feedstock material form and heat treatment," *Materials Today Communications*, vol. **34**, Art. no. 105156, (2023). https://doi.org/10.1016/j.mtcomm.2022.105156
6. Y. Bozkurt, A. Avşar, M. Korgancı, and G. Çam, "A comprehensive review on friction stir additive manufacturing of various structural alloys for aerospace applications," *Progress in Additive Manufacturing*, In-press, (2025). https://doi.org/10.1007/s40964-025-01160-y
7. A. Hassan, S. R. Pedapati, M. Awang, and I. A. Soomro, "A comprehensive review of friction stir additive manufacturing (FSAM) of non-ferrous alloys," *Materials*, vol. **16**, no. 7, p. 2723, (2023). https://doi.org/10.3390/ma16072723
8. R. S. Mishra, R. S. Haridas, and P. Agrawal, "Friction stir-based additive manufacturing," *Science and Technology of Welding and Joining*, vol. **27**, no. 3, pp. 141–165, (2022).https://doi.org/10.1080/13621718.2022.2027663
9. M. R. Roodgari, R. Jamaati, and H. Jamshidi Aval, "Fabrication of a 2-layer laminated steel composite by friction stir additive manufacturing," *Journal of Manufacturing Processes*, vol. **51**, pp. 110-121, (2020). https://doi.org/10.1016/j.jmapro.2020.01.031

10. Abhijit Datta, Ankit Shrivastava, Nilrudra Mandal, Himadri Roy, Shitanshu, Shekhar Chakraborty, “A comparative investigation of butt friction stir welding of aluminium alloys, AA1100 and AA7075, with AISI 304 stainless steel,” *Welding in the World*, vol. **67**, no. 6, pp. 1449-1465, (2023). https://doi.org/10.1007/s40194-023-01514-6
11. N.B. Dhokey, S.S. Maske, P. Ghosh, Effect of tempering and cryogenic treatment on wear and mechanical properties of hot work tool steel (H13), Materials Today: Proceedings, vol. **43**, no. 5, pp. 3006-3013, (2021). https://doi.org/10.1016/j.matpr.2021.01.361
12. A. Tamadon, A. Baghestani, and M. E. Bajgholi, “Influence of WC-Based Pin Tool Profile on Microstructure and Mechanical Properties of AA1100 FSW Welds,” *Technologies*, vol. **8**, no. 2, (2020). https://doi.org/10.3390/technologies8020034
13. H. Zuhailawati, M. N. Halmy, I. P. Almanar, A. A. Seman, and B. K. Dhindaw, “Mechanical Properties of Friction Stir Processed 1100 Aluminum Reinforced with Rice Husk Ash Silica at Different Rotational Speeds,” *International Journal of Metallurgical & Materials Engineering*, vol. **2**, no. 1, Jan. (2016). https://doi.org/10.15344/2455-2372/2016/120
14. A. R. Dixit, A. K. Srivastava, S. Dwivedi, A. Nag, and S. Hloch, “An investigation on microstructural features and bonding strength of magnesium-based multifunctional laminated composite developed by friction stir additive manufacturing,” *International Journal of Advanced Manufacturing Technology*, vol. **128**, no. 1-2, pp. 531-546, (2023). https://doi.org/10.1007/s00170-023-11911-2